PREPRINT UCRL- 76931

Lawrence Livermore Laboratory

UNIFICATION OF TERMINOLOGY CONCERNING THE ERROR MOTION OF AXES OF ROTATION

J. B. Bryan

P. Vanherck

June 20, 1975

This paper was prepared for publication in the Annals of the CIRP and for presentation at the Annual Meeting of CIRP, Freudenstadt, West Germany, August 24-30, 1975.

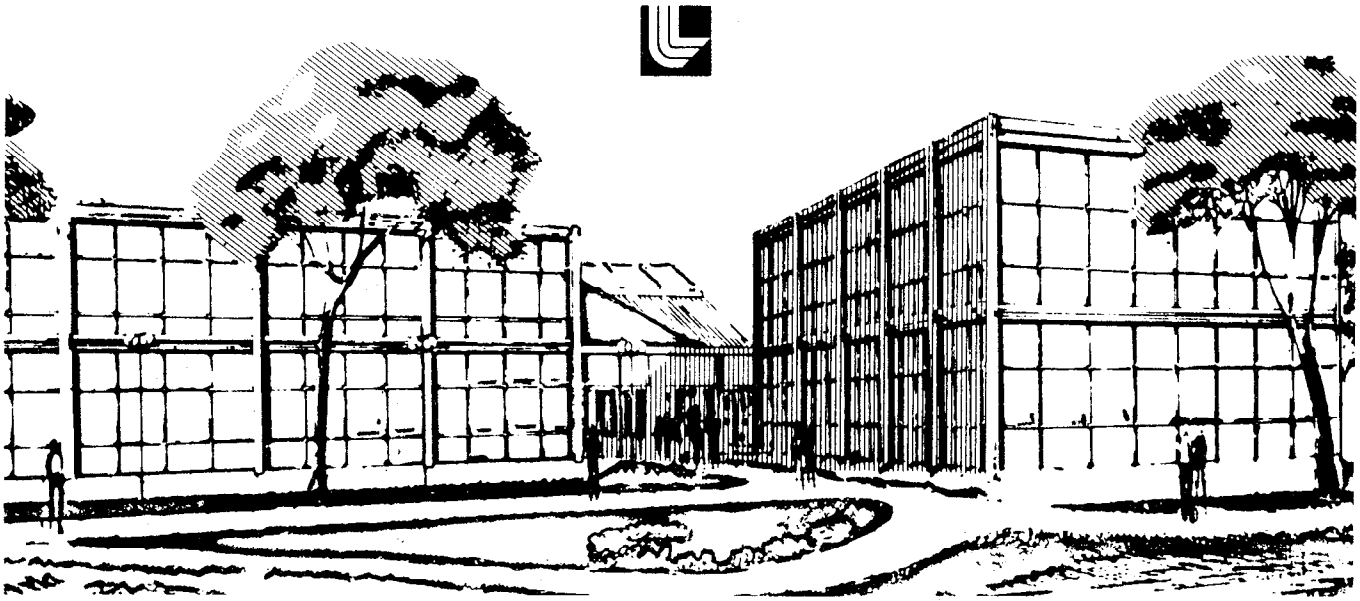

UNIFICATION OF TERMINOLOGY

CONCERNING THE ERROR MOTION OF AXES OF ROTATION*

J. B. Bryan, Lawrence Livermore Laboratory (1)
P. Vanherck, Catholic University of Leuven (2)

Synopsis

Existing terminology for the description of the truth of axes of rotation of spindles is inadequate to meet the current needs of science and industry. This paper provides an introduction to a new terminology unification document that establishes a coherent language for dealing with this subject. The new document is the result of a cooperative effort of the CIRP Scientific Technical Committee Me and is based on a draft of the American National Standards Institute Committee B89.3.4.

J. B. Bryan (76931)
c/o Technical Information Department
University of California
Lawrence Livermore Laboratory
Livermore, California 94550

*This work was performed under the auspices of the U.S. Energy Research & Development Administration.

I. Introduction

The measurement of error motion of the axes of rotation is an important item in the geometrical accuracy of machine tools and measuring machines. However, it has not been treated explicitly in the tests proposed by Schlesinger or Salmon, or in the ISO Recommendation R 230.

The first methods developed for the measurement of this error motion have been described by J. Tlusty [1] in 1959 and by J. B. Bryan in 1967 [2]. A subgroup of the Scientific Technical Committee Me was formed in 1972 at the suggestion of J. B. Bryan to compose an unambiguous formulation for the measurement and evaluation of the error value. The subgroup's task was to draw up a unification document on terminology and measuring methods concerning the error motions of axes of rotation. The ANSI draft standard, "Axes of Rotation," sponsored by the American Society of Mechanical Engineers, was used as the basic document for the discussion [3]. Comments were received from members from Belgium, France, Germany, Netherlands, Poland, Switzerland, Czechoslovakia, and the USA. In the General Assembly in 1975 the final version of this document was approved by the Scientific Technical Committee Me.

The scope of the unification document is:

- The unification of methods of describing and testing axes of rotation found in machines to produce, measure, or handle manufactured products.

- Specification and measurement criteria that consider the functional use of the axis and permit a meaningful description of the axis as it performs its actual function.

The instrumentations for testing error motion are not considered in the document.

In addition to the work of the Scientific Technical Committee, an increasing number of industrial people are evaluating the axes of rotation of their machines. However, many erroneous measuring procedures are used. For example, in many places the radial error motions of lathes are defined with the two perpendicular gauges method. Also the evaluation methods differ from place to place.

The goal of this paper is to show, with some actual examples, the general philosophy of the unification document.

2. Arguments for Measuring the Error Motion of Axes of Rotation

Consider a cylindrical cutting operation on a lathe, using an ideal cutting tool that is capable of cutting in exact accordance with its position without deflection or wear and that has a flat nose with a width equal to the longitudinal feed per revolution. A perfect cylinder would be cut if the axis of rotation remained parallel to the feed motion and stayed a constant distance from the tool nose. However, if the distance between the axis of rotation and the tool changed (due to a geometrical error in the front bearing, for example), the workpiece would present geometrical form deviations. The variation in the distance between the axis of rotation and the tool is called the *error motion of the axis of rotation* in this paper.

When the error motion is not at all repetitive, i.e., when it is purely random, the out-of-roundness of the cylinder, measured over a sufficient number of feed-marks, is practically zero; however, the workpiece does show roughness.

The functional behavior of the produced part can be strongly influenced by the geometrical deviations, out-of-roundness, undulations, and roughness. Therefore it is indispensable, for characterizing the geometrical accuracy of a machine tool, to measure and describe in a unique manner, the error motion of the axis of rotation (see Fig. 1).

Similar arguments can be given for most other cutting operations and many measuring devices.

3. Sensitive Directions

The motion of the axis of rotation, as well as the motion of the tool post, can generate geometrical form deviations in the produced cylinder. However, when both motions are identical, for

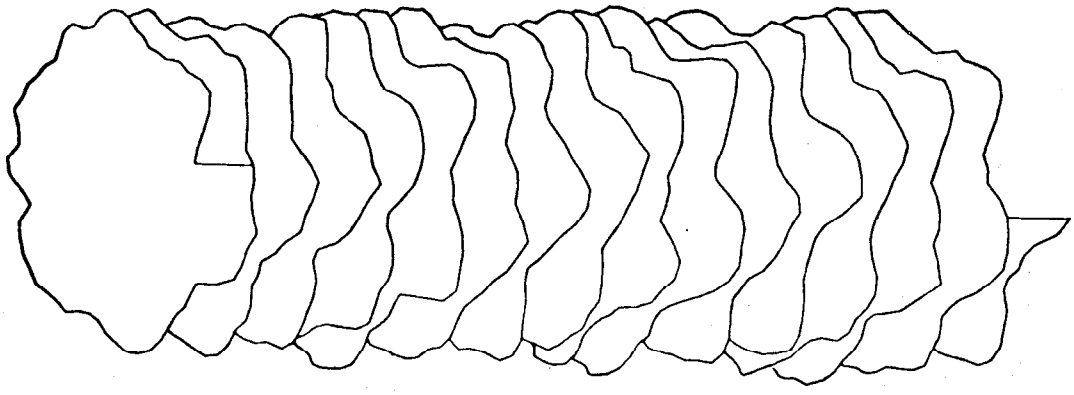

Fig. 1. Three-dimensional representation of the geometrical deviations due to an axis-of-rotation error motion.

example, in a lathe mounted on board a rolling ship, the workpiece accuracy is not influenced. Thus, what is important is the *relative motion* between the axis of rotation and the tool. It involves only the *structural loop*, i.e., the mechanical components which maintain the *relative position* between the workpiece and the tool.

Only one component of the relative motion has to be considered. In the cylinder cutting operation, a relative motion in

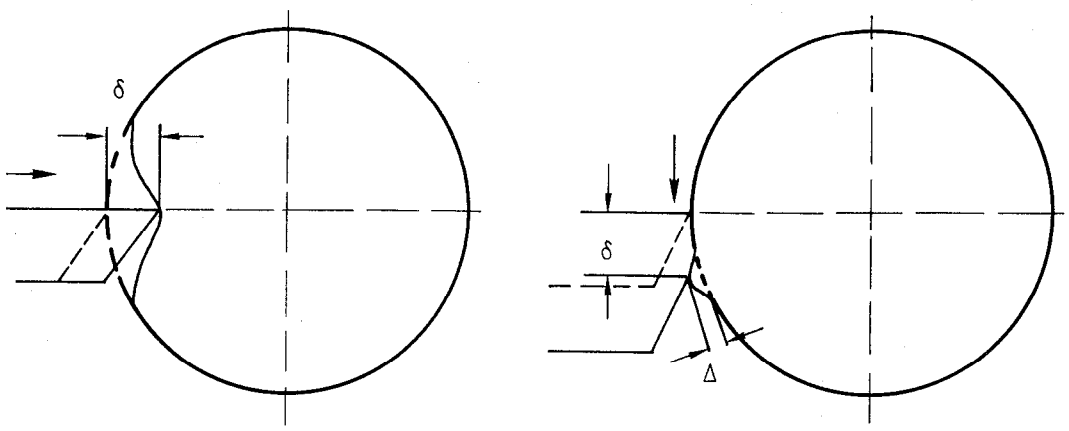

Fig. 2. Error due to relative motion in (a) sensitive direction (one-for-one error) and (b) nonsensitive direction (second order error).

the radial direction cuts a one-for-one form error into the workpiece. Hence, this radial direction is called a *sensitive direction* (Fig. 2a).

A relative motion in the feed direction does not influence the geometrical precision, and the influence of a relative motion in the cutting speed direction is only of second order consequence and can be neglected. Hence, these two motions are in a *nonsensitive direction* (Fig. 2b).

From these concepts the following general definitions have been developed:

- The sensitive direction is parallel to a line perpendicular to the ideal generated workpiece surface through the instantaneous point of machining or gauging.
- A non-sensitive direction is along any line perpendicular to the sensitive direction.

Two types of sensitive directions are recognized: the fixed and the rotating sensitive directions. In the fixed sensitive direction, the workpiece rotates with the axis of rotation and the point of machining or gauging is fixed. Examples of fixed sensitive directions are shown in Fig. 3 for some turning operations. In the rotating sensitive direction, the workpiece is fixed and the point of machining or gauging rotates with the axis. Figure 4 illustrates the rotating sensitive direction at two instants in time in jig boring a hole.

4. Fixed Sensitive Direction (Rotating Workpiece)

4.1 Radial Sensitive Direction

4.1.1 Principle

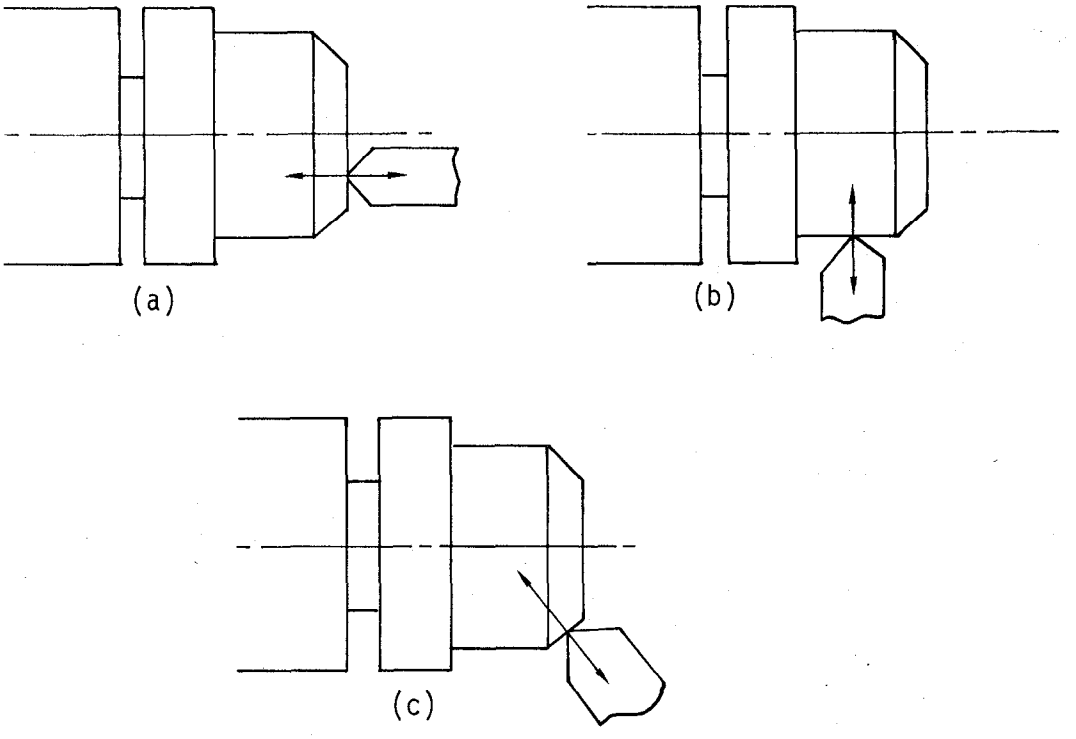

Fig. 3. Sensitive direction in (a) facing, (b) turning, and (c) chamfering (taken from Ref. 3).

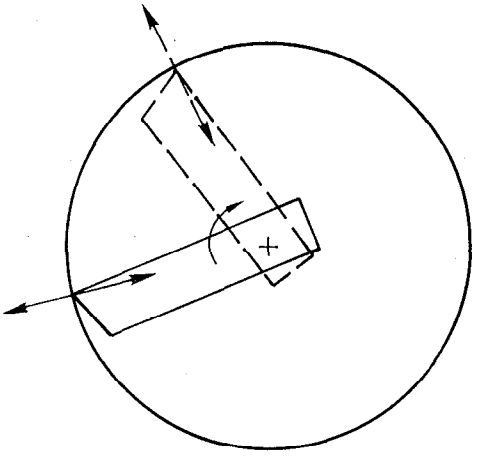

Fig. 4. Rotating sensitive direction at two instants in time in jig boring a hole (taken from Ref. 3).

In a groove-plunging operation (Fig. 5) the sensitive direction is along a radial line going through the tool nose. The relative displacement between the axis of rotation and the tool, measured along this radial line, is called the radial motion in that particular axial position.

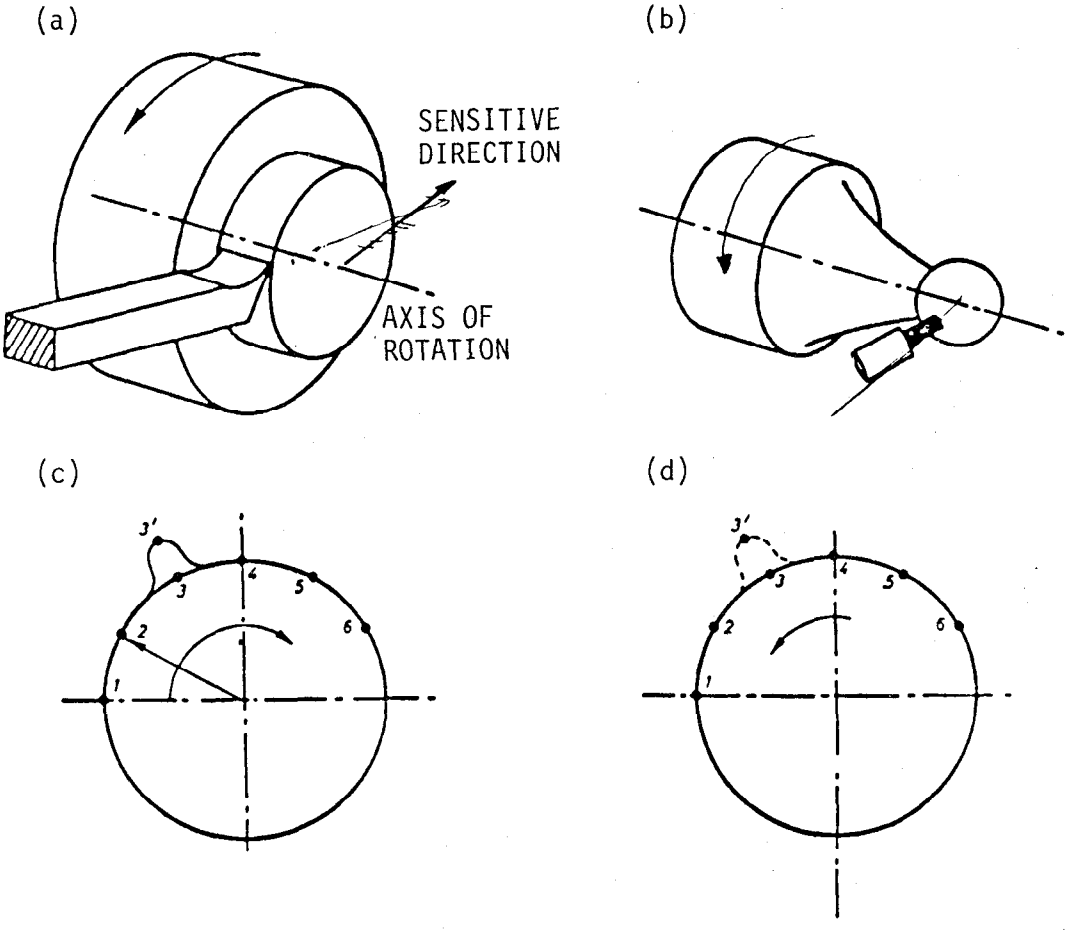

Fig. 5. Radial plunge turning: (a) plunging operation; (b) measuring set-up; (c) figure on the screen; (d) section of the workpiece.

The test setup for measuring this radial motion generates on the screen of an oscilloscope a vector rotating in synchronism with the spindle. The end point of the spindle appears as a bright spot on the screen. The length of the vector is modulated by the motion signal, which is detected by a noncontact displacement transducer mounted on the tool post. The transducer measures the gap between its sensitive surface and a spherical master fixed on the spindle (Fig. 5b).

If no error motion were detected, the image on the screen would be a perfect circle, and the part produced with an ideal cutting tool would be a perfect cylinder.

However, if at the moment t_3 the distance between the axis of rotation and the gauge increases, a hill will be drawn on the screen (Fig. 5c). A machined workpiece (Fig. 5d) would also present a hill at that particular place (i.e. point 3).

To be consistent with the International Standards, the unified document recommends considering a motion of the axis of rotation towards the tool as positive. However, to simplify the comparison between the measured error motion of an axis of rotation and the out-of-roundness of the workpiece machined on this axis, the sign convention for roundness measurement is used in this paper. Thus, an increase in the distance between the axis of rotation and the tool, which generates a hill on a workpiece, also generates a hill on the screen of the oscilloscope. Hence, by taking the scales into account, the figure on the screen of the oscilloscope corresponds to the best workpiece roundness the machine is capable of producing under ideal cutting conditions at the considered rotational speed of the spindle.

When the spherical master is perfectly concentric with the average position of the axis of rotation, the figure on the screen is called an error motion polar plot. Generally the picture of the screen will be taken over several revolutions with a camera attachment.

The capability of the method will be demonstrated with an example. To choose the optimum machine for the production of a precision element, we analyze the error motion polar plots of the workpiece spindles of the available cylindrical grinding machines as described below.

Figure 6 shows an error motion polar plot from a 5-year-old machine. As the pattern of the polar plots are identical for all rotational speeds, the origin of the error motion was looked for in the bearing itself. It was found that, due to a bad bearing seal, grinding dust penetrated the front bearing, causing

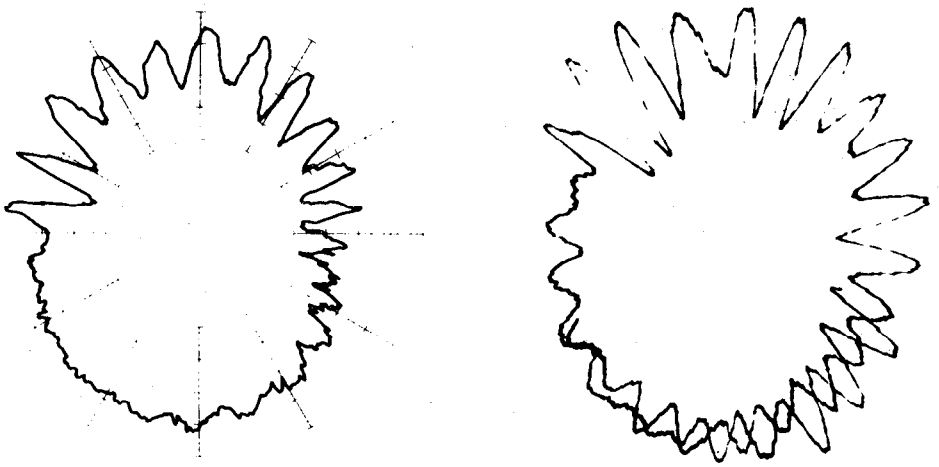

Fig. 6. Cylindrical-grinding machine: (a) polar plot showing error motion of the workpiece spindle; (b) polar plot showing workpiece out-of-roundness.

wear with a wavy pattern in the outer ring of this bearing. Figure 6b shows that the polar plots of the out-of-roundness of the workpieces produced on this cylindrical grinding machine have the same shape as the error-motion polar plot on the screen of the oscilloscope.

4.1.2 Generation and Modulation of the Rotating Vector

As oscilloscopes with polar inputs are generally not available, the rotating vector can be obtained by applying sine and cosine signals generated by the rotation of the spindle, to the X and Y inputs of a common oscilloscope.

In the method described by Bryan, et al. [2], these two signals are generated by two circular cams, eccentric by 0.725 mm in perpendicular directions. The cams were mounted on the spindle and sensed by two gauges (Fig. 7a).

In the method described by Vanherck and Peters [4], a small (57 g) commercial vector resolver unit is physically attached to the axis of rotation, the rotor of which is fed by a carrier signal. Demodulating and filtering the resolver output yields the sine and cosine signals (Fig. 7b). Multiplying these sine and cosine signals by the error motion signal yields the length modulation of the rotating vector. To get a true image of the out-of-roundness of the machined workpiece, it is necessary to reverse the rotation of the vector on the screen with respect to the rotation of the spindle (Figs. 5c and 5d). On the screen the workpiece is presented as stationary, but on a grinder or lathe it is rotating.

4.1.3 Compensation for the Spherical Master's Eccentricity

Figure 8 shows that, even when the geometrical axis of the workpiece blank does not coincide with the axis of rotation, a perfect cylindrical part could be machined if the error motion of the axis of rotation were zero. This is only true, however, if second order effects, such as unbalance, are ignored. Thus, an eccentricity of the workpiece blank with respect to the spindle is of no consequence.

On the other hand, the spherical master should theoretically be perfectly centered on the axis of rotation. Although the sphere is mounted on a special adjustable rig, it is impossible to center it perfectly by mechanical means. When the value of this eccentricity is of the same order or larger than the error motion, the figure on the screen could be deformed as shown in Fig. 9. This deformation is called a limacon and could be misinterpreted as an error motion.

Both previously described methods provide an electronic compensation of the master ball eccentricity, by adding an adjustable amount of sine and cosine components to the gauge signals.

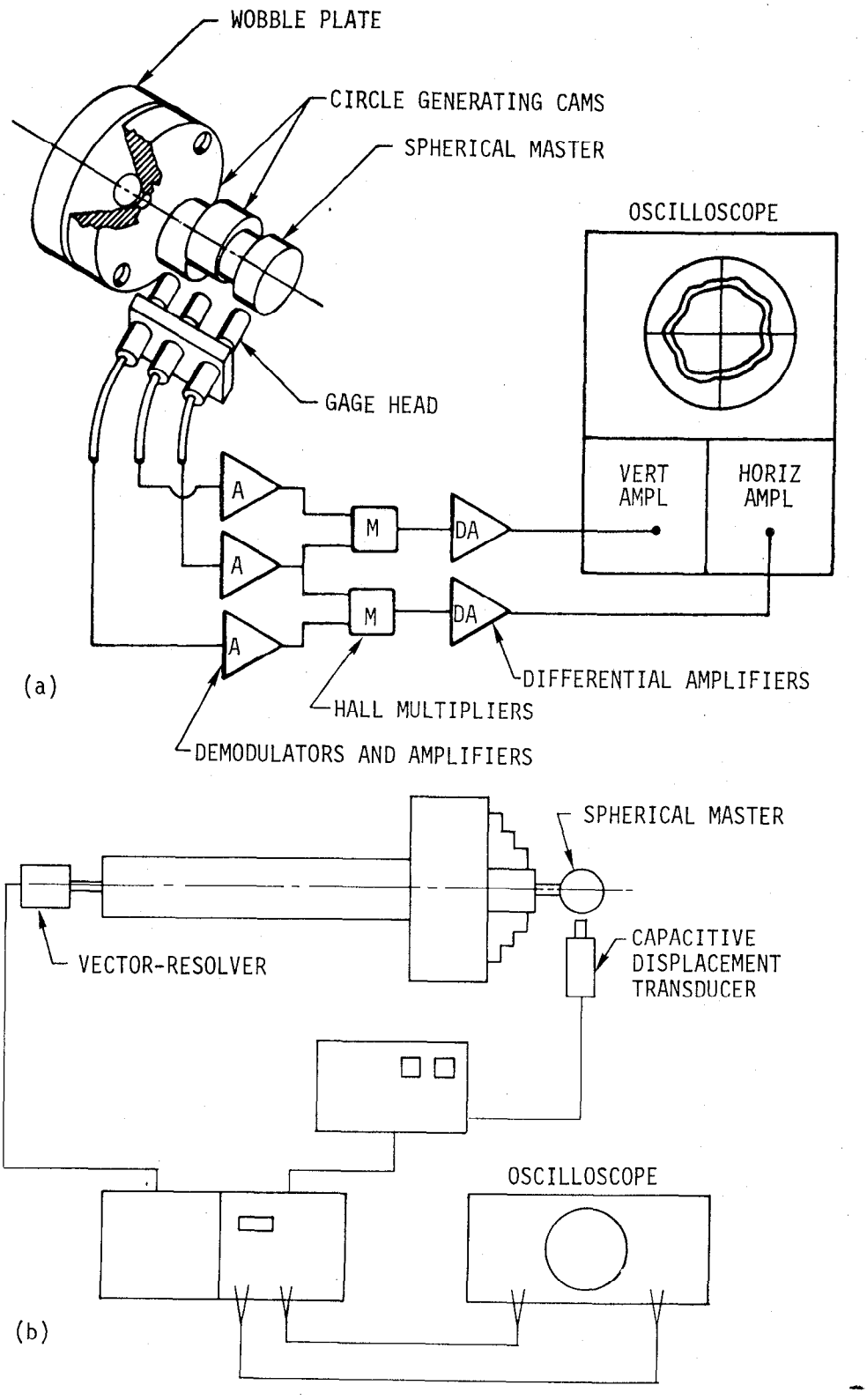

Fig. 7. Generation of the rotating vector: (a) two cams methods (Bryan); (b) vector resolver method (Vanherck).

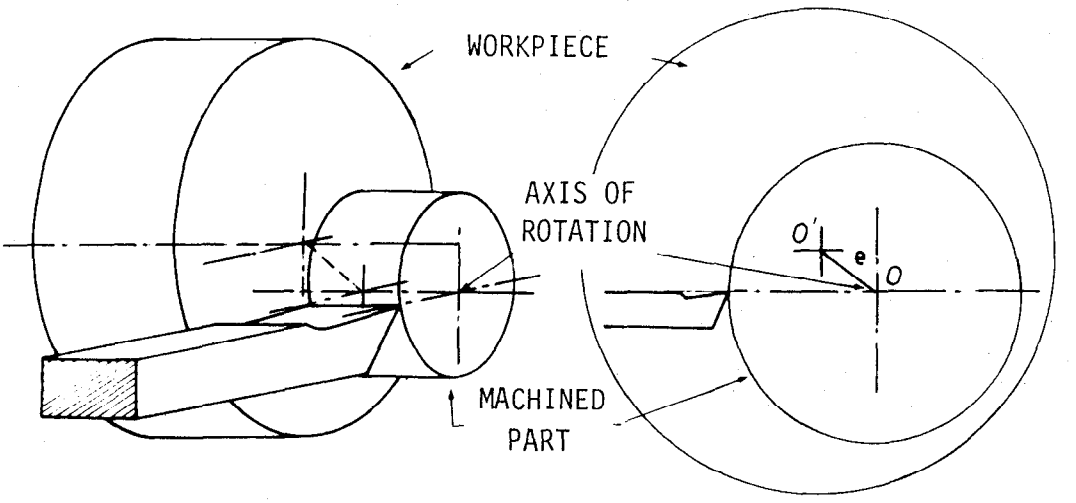

Fig. 8. Machining of eccentric workpiece.

Fig. 9. Deformation of the polar plot due to the eccentricity of the sphere.

4.2 Axial and Angular Motions

In a face-cutting operation on a lathe, the departure from flatness ($\overline{KM}$) at a given point K on the workpiece, can be decomposed into two components, $\overline{KL}$ and $\overline{LM}$ (Fig. 10).

The component $\overline{KL}$ is equal to an axial motion $z(t)$ in which the axis of rotation remains coaxial with its average position and moves axially with respect to it.

The component $\overline{LM}$ is due to the angular motions $\alpha(t)$ in which the axis of rotation moves angularly with respect to its

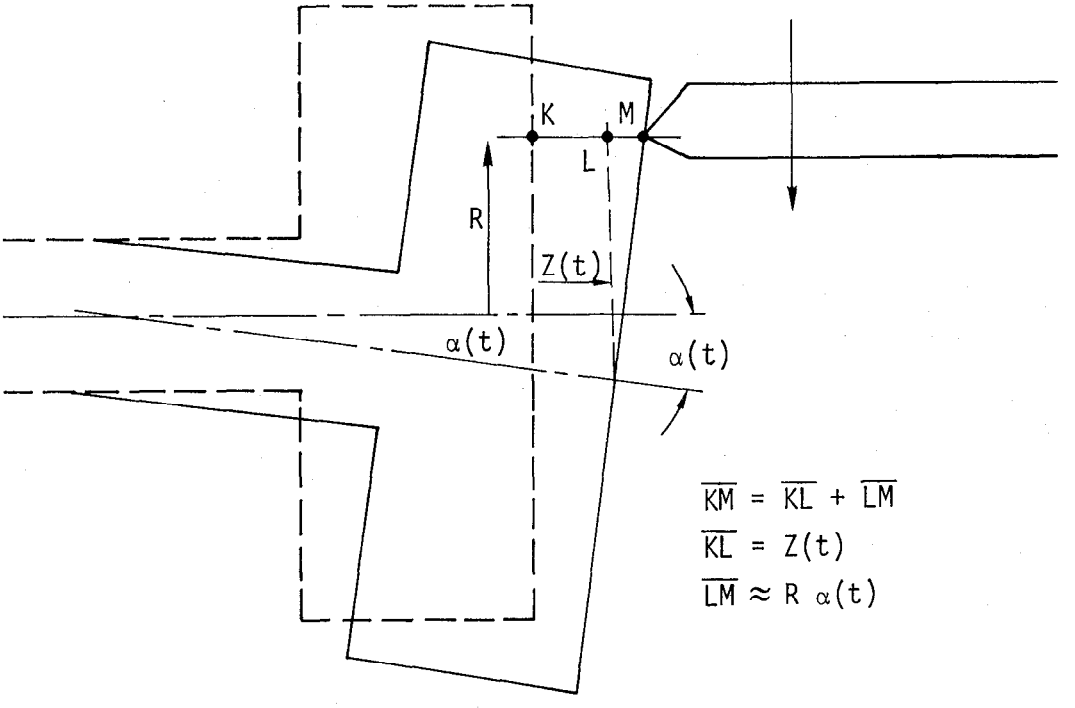

Fig. 10. Error motion in face cutting (taken from Ref. 3).

average position in the plane of the axial and radial motions. As the angular motion $\alpha(t)$ is very small, the motion component $\overline{LM}$ can be assumed equal to the product of the angular motion and the radius R to the considered point K:

$$LM \approx \alpha(t)R.$$

The axial motion can be measured with the apparatus shown in Fig. 11, and can be displayed in a polar plot by the same electronic circuit as described for the radial motion. However, as shown by Fig. 12, a once-per-revolution sinusoidal motion causes a departure from flatness. This once-per-revolution sinusoidal component, should not be compensated; it is a part of the error motion to be measured.

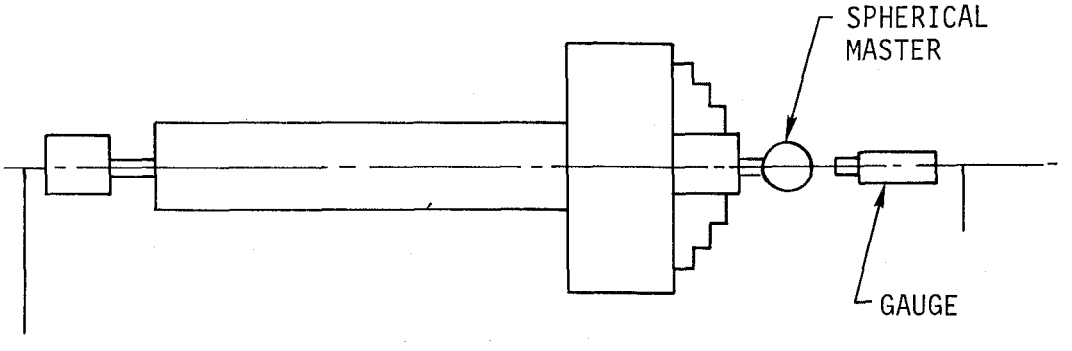

Fig. 11. Measuring setup for axial motion.

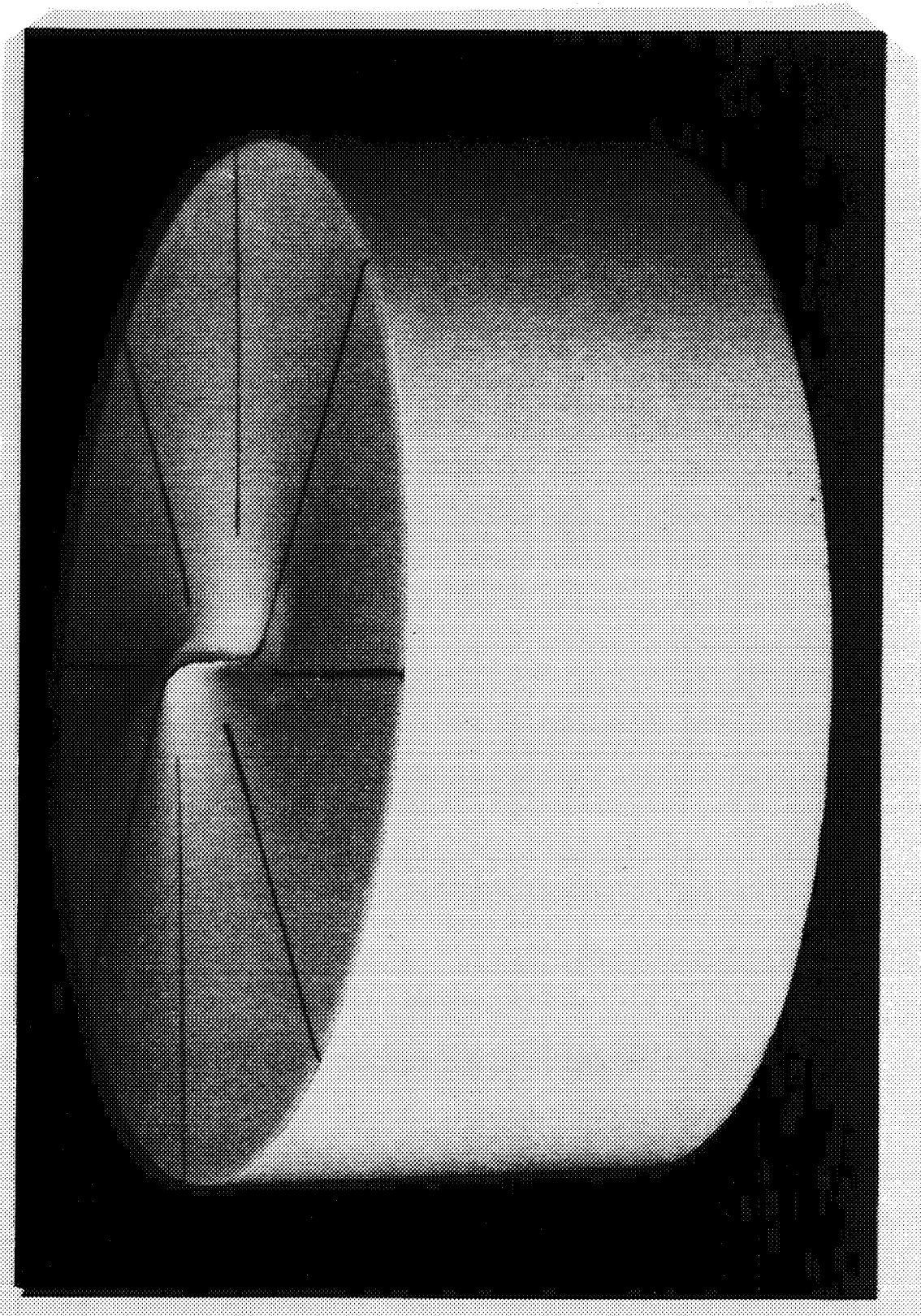

Fig. 12. Effect of fundamental motion on a face cutting operation.

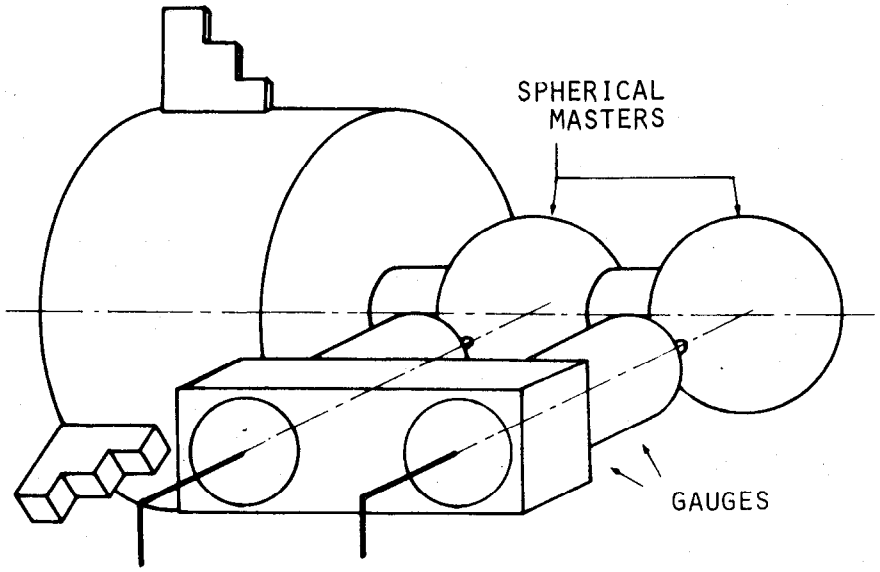

Fig. 13. Measuring setup for angular motion.

The angular motion can be measured using the arrangement shown in Fig. 13. The two spherical masters, separated by a distance L, have to be mounted as concentric as possible with respect to the axis of rotation.

The angular motion can be deduced from the difference in the output signals of the gauges,

$$\alpha(t) = \frac{X_1(t) - X_2(t)}{L}, \qquad (1)$$

and can be displayed and compensated in the same way as for the radial motion.

5. Evaluation of the Motion Plots

After the pictures of the motion polar plots have been taken, the error motions have to be expressed in unambiguous values.

5.1 Error Motion Polar Plots

Polar plots taken over several spindle rotations for radial and axial motions are known as total error motion polar plots (Fig. 14).

When a cylinder is machined on a lathe, using an ideal cutting tool with large nose radius, the out-of-roundness of the part is determined by the locus of the *smallest* distances between the tool nose and the axis of rotation. On the picture of the screen this corresponds to the contour of the inner boundary of the total error motion polar plot, which is referred to as the inner error motion polar plot.

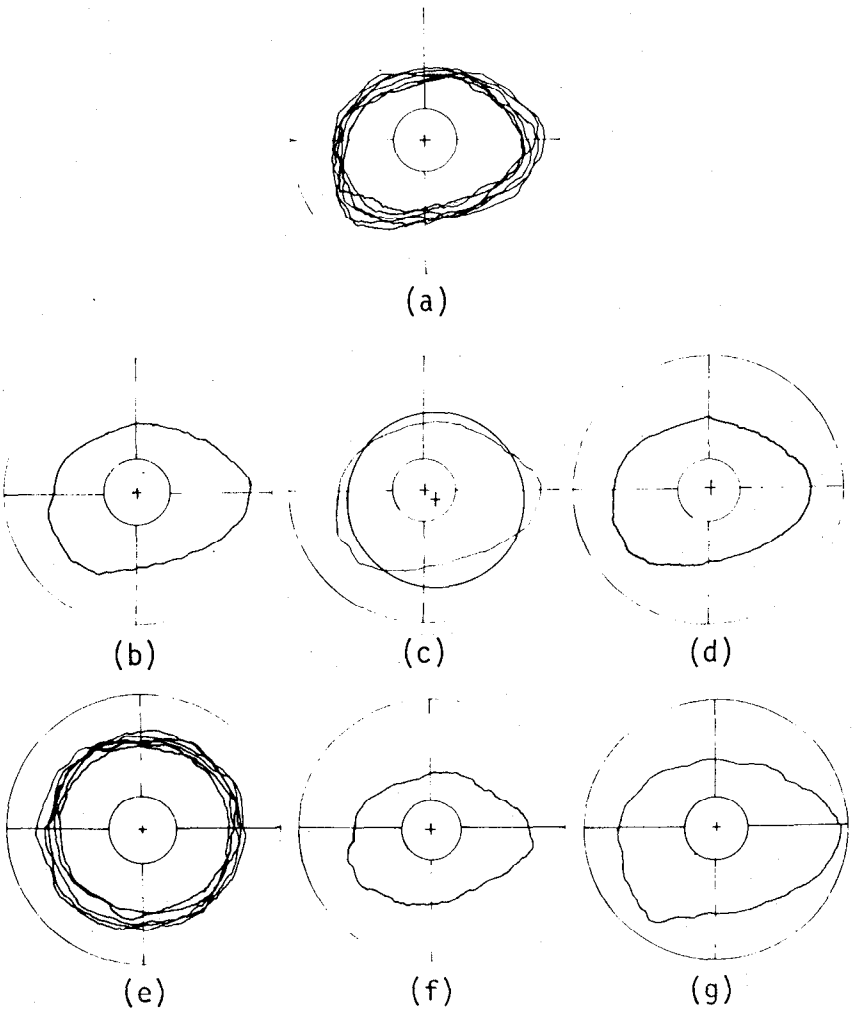

Fig. 14. Polar plots of error motion: (a) total error motion; (b) average error motion; (c) fundamental error motion; (d) residual error motion; (e) random error motion; (f) inner error motion; (g) outer error motion.

When with a similar tool a hole is machined by jig boring, the out-of-roundness of the part is determined by the locus of the largest distances between the tool nose and the axis of rotation. On the total error motion polar plot this can be represented by its outer boundary and is referred to as an outer error motion polar plot.

The error motion component, which is repetitive from revolution to revolution, can be defined by averaging the error motion polar plot at each angular position over the number of recorded revolutions. This polar plot is called an average error motion polar plot.

The roughness of the machined part is directly influenced by the motion components being nonrepetitive from revolution to

revolution. This random error motion polar plot is defined as the deviation of the total error motion polar plot from the average error motion polar plot.

It has been shown above that the once-per-revolution component of the axial error motion may not be compensated. On the polar plot this component is represented as the offset of the best-fit circle passing through the average error motion polar plot, and is known as the fundamental error motion polar plot.

The difference between the average and the fundamental error motion polar plot is defined to find the sources of the axial error motion. It is known as the residual error motion polar plot.

5.2 Error Motion Values

The evaluation of an error motion polar plot (this means the expression of the error motion in an unambiguous value) will be done by a procedure similar to the one used in the evaluation of out-of-roundness.

The error motion value is the scaled difference in radii between two concentric circles from a specified center just sufficient to contain the considered error motion polar plot.

The polar chart center (P.C.) on the screen of the oscilloscope is the center about which the vector rotates.

The evaluation about a center not coinciding with the polar chart center has, in a first approximation, the same effect as a compensation of a once-per-revolution sinusoidal component of the error motion. This means that the small residual once-per-revolution component, due to an imperfect electronic compensation of the spherical master eccentricity, can be eliminated by evaluating the error motion's value from an appropriate center.

However, for axial error motion, the once-per-revolution sinusoidal component may not be eliminated, this axial error motion *has to be* defined from the polar chart center.

For the radial and angular error motions, one of the following centers can be chosen:

- The maximum inscribed circle center (M.I.C.).
- The minimum circumscribed circle center (M.C.C.).
- The least squared circle center (L.S.C.).
- The minimum radial separation center (M.R.S.).

The specification of a measurement should at least contain the type of error motion polar plot that has been considered and the center from which the evaluation has been carried out. For example, for an axial error motion the total error motion value about the polar chart center could be defined. This means the scaled difference in radii between two concentric circles from the polar chart center, just sufficient to contain the total error motion polar plot. For cylindrical cutting on a lathe, the inner

error motion value about the maximum inscribed circle center could be evaluated, etc.

There is only one exception to this general rule. The random error motion is not defined as the difference in radii between two concentric circles, but as the scaled width of the total error motion polar plot, measured along a radial line through the polar chart center.

6. Examples of Radial Error Motion Polar Plots

Figures 15 through 17 show some typical radial error motion plots from lathes. Figures 15a and 15b are plots of a 7-kW lathe with a plain bearing spindle. For high speeds (375 rpm) the error motion is small, as shown in Fig. 15b. Figure 15a, taken at a rotational speed of 30 rpm shows that the speed was not high enough to form a stable oil film in the bearing.

Figure 16a and b show the error motion of a spindle on conical roller bearings, from a 2-kW lathe at the same rotational speed (600 rpm). In Fig. 16a the spindle was driven by a belt, whereas in Fig. 16b it was driven by a gear drive. The influence of the drive can easily be detected from the polar plots.

It is possible to insert a low-pass filter in the electronic circuit to eliminate the high frequency components. A nice application of these filters is shown in Fig. 17. The radial error motion of this 3-kW lathe is the resultant of two components, one of a structural deformation at 135 Hz due to vibration and one due

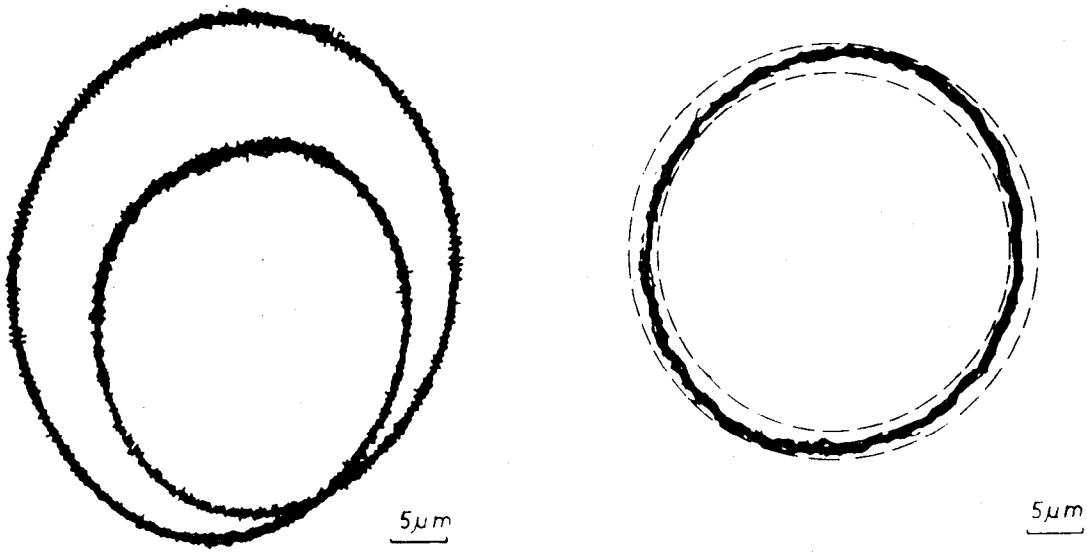

Fig. 15. Polar plot of radial error motion from a spindle on plain bearings at (a) 30 rpm and at (b) 370 rpm.

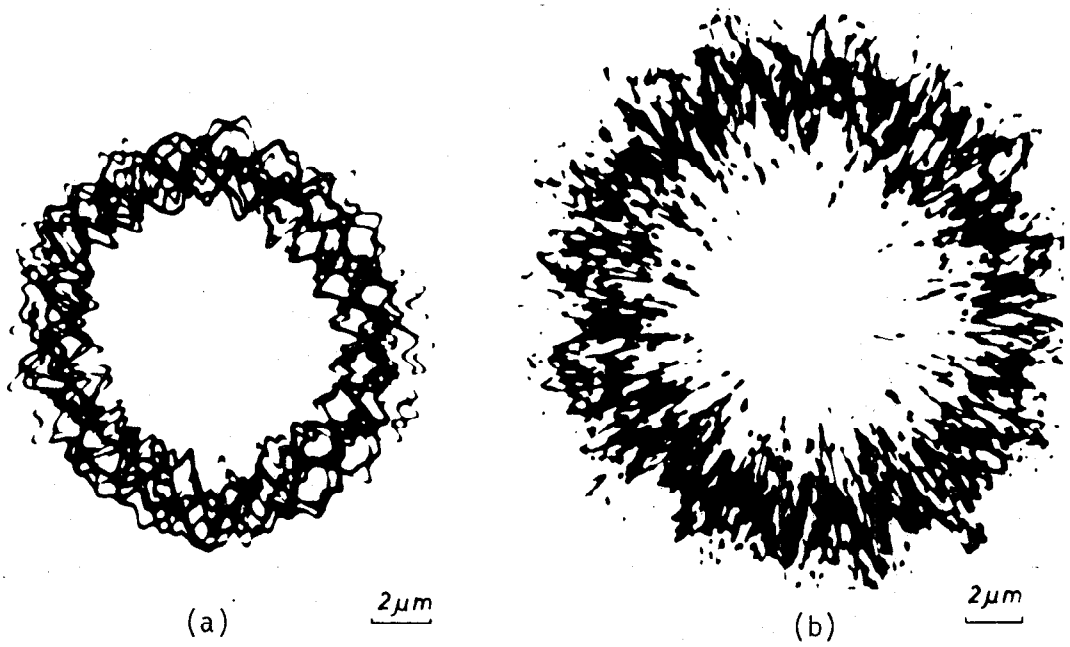

Fig. 16. Polar plot of radial error motion from a spindle (a) driven by a belt and (b) driven by a gear drive.

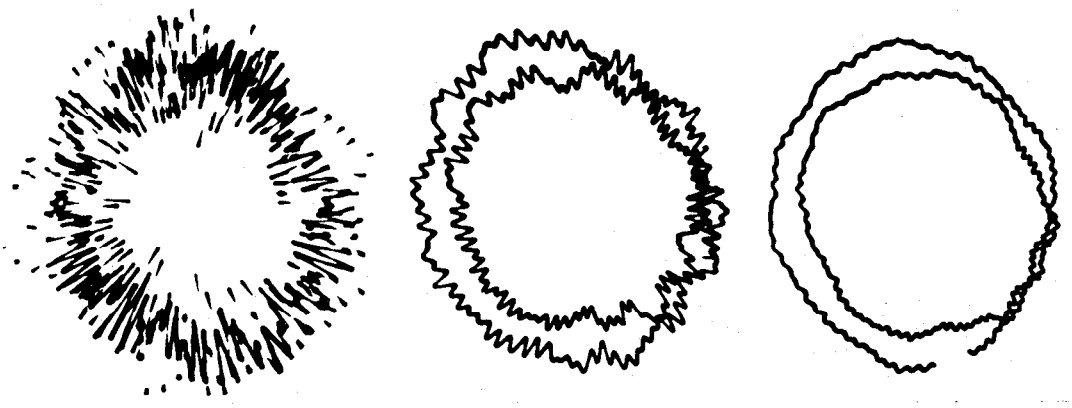

Fig. 17. Example of using a low-pass filter to filter the components of the structural vibrations: (a) unfiltered; (b) partially filtered; (c) almost all filtered.

to a geometrical error in the conical front bearing. In Fig. 17b and c, the components of the structural vibrations are gradually filtered out. The image shifts but reproduces its shape in somewhat more than two revolutions. This error is due to one roller having a slightly larger diameter than the average one, causing one error motion with a frequency of 0.43 of the spindle rotational frequency. The influence of the structural error motion is nicely shown in Fig. 17a, which is taken without filtering. In Fig. 17c the 135 Hz motion component was almost completely filtered out and shows perfectly the error motion component due to the improper bearing roller.

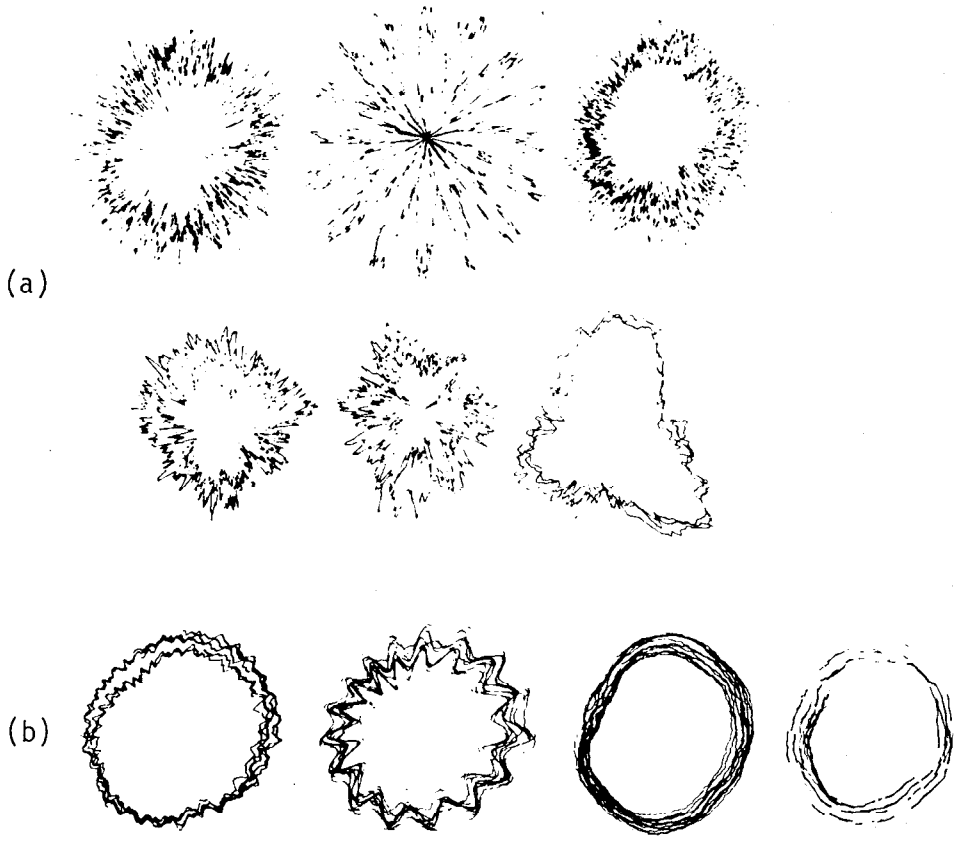

Fig. 18. Error motion plots of a precision lathe (a) without filter and (b) with filter.

Figure 18 shows some radial error motion polar plots of a high precision lathe with continuous speed variation. The men in the workshop knew that the parts machined on this lathe sometimes presented a significant out-of-roundness, even when a flat-nose tool was used. A systematic analysis showed that high error motion values were detected at 1760 rpm, 880 rpm, 330 rpm, etc.

For 330 rpm the polar plot showed 16 lobes, for 880 rpm six lobes, and for 1760 rpm three lobes. It was found that the spindle had a low-damped natural frequency of 88.2 Hz. Each time this natural frequency coincides with a multiple of the numbers of revolutions per second, high error motions are generated.

The computations have been summarized in Table 1. Some of the polar plots have also been taken with a low pass filter, reducing the 88.2 Hz component to 10% of its initial value (Figs. 18g to j). From these filtered plots, we can deduce that an appropriate damping of this spindle would drastically increase the machine's capability of producing parts with low out-of-roundness errors.

Table 1. Computation concerning the error motion polar plots of Fig. 18.

Rotation rpm (rps)	Polar plot: Without filter	Polar plot: With filter	Excited frequency
168 (2.80)	a	g	X32 = 89.6
332 (5.53)	b	h	X16 = 88.5
363 (6.05)	c	i	X14 = 84.7 X15 = 90.75
725 (12.08)	d	j	X7 = 84.56 X8 = 96.64
880 (14.66)	e		X6 = 87.9
1760 (29.33)	f*		X3 = 87.9

*The scale of polar plot f is half the scale of the other polar plots.

7. Digital Evaluation of Radial Error Motion Values

In the analog method, the evaluation of the error motion has to be carried out by tracing circles on the picture of the oscilloscope. Although this method is valuable for most industrial applications, it can be proven that a direct digital measurement of the motion and the computation of the error motion value by a digital computer has many advantages.

The capability of this method will be demonstrated with some examples. The radial and axial error motions of two, three-year-old 2.5-kW production lathes will be compared. Both machines were produced by the same manufacturer and have the same dimensions. However, the spindle of lathe G is mounted on radial plain bearings whereas lathe J has conical roller bearings. There is also a difference in the speed range of both machines.

The radial error motion of the lathe on plain bearings, for a rotational speed of 90 rpm, is shown in Fig. 19. The total radial motion, without compensation for the residual eccentricity of the spherical master, is shown in the left upper corner. The end point of the arrow shows the position of the least square circle center (L.S.C.). Instead of tracing circles around this L.S.C., the corresponding once-per-revolution sinusoidal component has been removed digitally from the motion signal. After this transformation the least squares circle center coincides with the origin of the polar coordinates system. This yields the total error motion polar plot shown in Fig. 19b. The difference between the radii of two concentric circles from the L.S.C., just sufficient to contain the total error motion polar plot, is 2.37 μm.

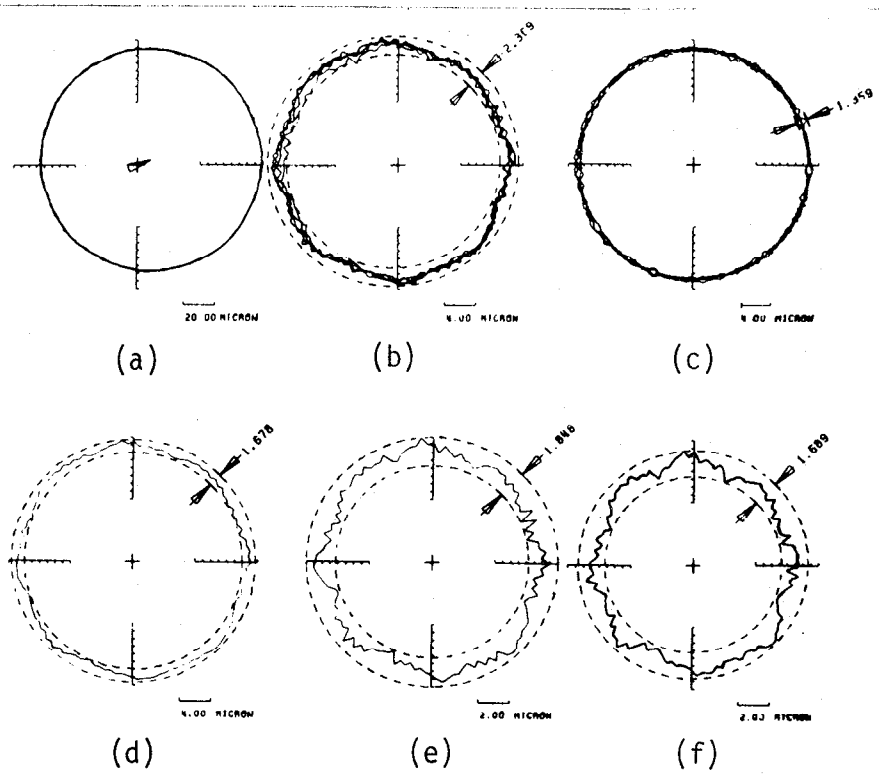

Fig. 19. Polar plots showing radial error motion of a spindle rotating at 90 rpm on plain bearings, fundamental amplitude = 8.92 and fundamental phase = 20.33: (a) total motion; (b) total error motion; (c) random error motion; (d) average error motion; (e) outer error motion; (f) inner error motion.

Also, the inner, outer, average, and random error motion polar plots were traced. The following error motion values from the L.S.C. can be evaluated: outer error motion value = 1.8 μm, inner error motion value = 1.5 μm, average error motion value = 1.6 μm, and random error motion value = 1.3 μm.

The axial error motion of the same lathe at the same speed is shown in Fig. 20. Since the fundamental component may not be compensated, the total error motion is evaluated from the polar chart center. The total error motion value is 11.5 μm.

The outer and inner error motions are respectively, 10.2 μm and 10.4 μm, which are several times larger than the corresponding values in the radial direction. These significant values are due to the once-per-revolution sinusoidal motion component. Indeed, the scaled distance from the polar chart center to the least square center, indicated by the end point of the arrow in Fig. 20a, is 4.15 μm, which corresponds with a fundamental error motion of 8.3 μm. This motion can easily be explained by an out-of-squareness of the axis bearing.

Figure 20 also shows that the residual error motion, which is the difference between the average and the fundamental error motions, is composed of an ovality and an eight lobed figure. This component is due to a natural frequency of 12 Hz for the lathe on its foundation.

The random error motion, which is the difference between the total and the average error motion, shows a once-per-two-revolutions component. This component is due to a slightly larger diameter of one of the balls of the axial bearing.

The radial error motion of the lathe on conical roller bearings is shown in Fig. 21. The total error motion (about 7 μm) is large with respect to the average motion (1.7 μm). This is due to a once-per-2.3-revolutions component caused by a larger diameter of one of the conical rollers of the front bearing.

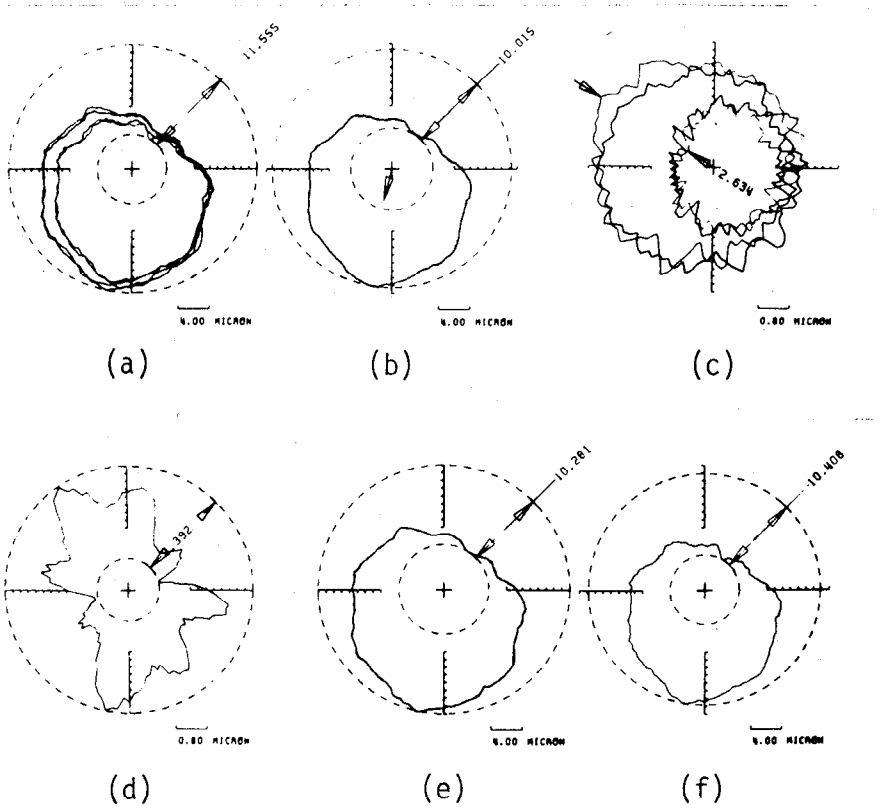

Fig. 20. Polar plots showing axial error motion of a spindle rotating at 90 rpm on plain bearings, fundamental amplitude = 4.15 and fundamental phase = -104.60: (a) total error motion; (b) average error motion; (c) random error motion; (d) residual error motion; (e) outer error motion; (f) inner error motion.

The total axial error motion, shown in Fig. 22, has a low value (about 2.2 μm) with respect to the radial motion. The distance from the P.C. to the L.S.C. is 0.71 μm. This means that an important part of the axial average motion is due to the fundamental motion (1.42 μm) caused by the nonsquareness of the bearings with respect to the axis of rotation. The random motion, with a value of 0.76 μm, is due to dynamic structural deformations.

This example proves that the axis of rotation measurement is not only valuable for the characterization of the machine tool's capability of producing workpices with low geometrical form errors, but is also powerful in tracing back the sources of the different error motion components.

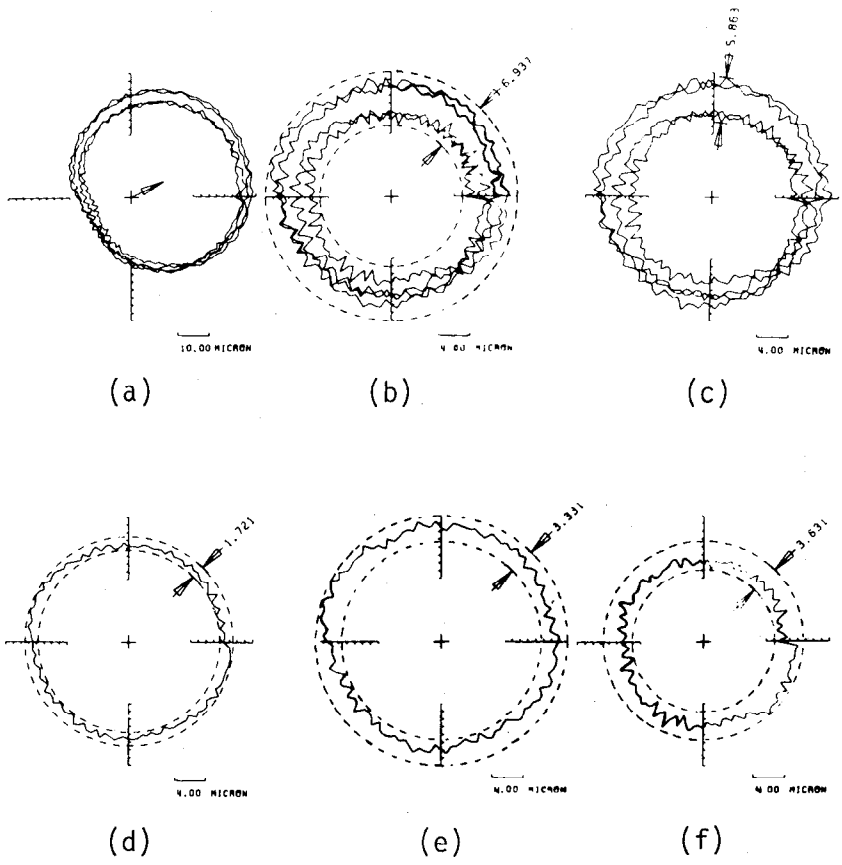

Fig. 21. Polar plots showing radial error motion of a spindle rotating at 180 rpm on conical roller bearings, fundamental amplitude = 11.69 and fundamental phase = 26.95: (a) total motion; (b) total error motion; (c) random error motion; (d) average error motion; (e) outer error motion; (f) inner error motion.

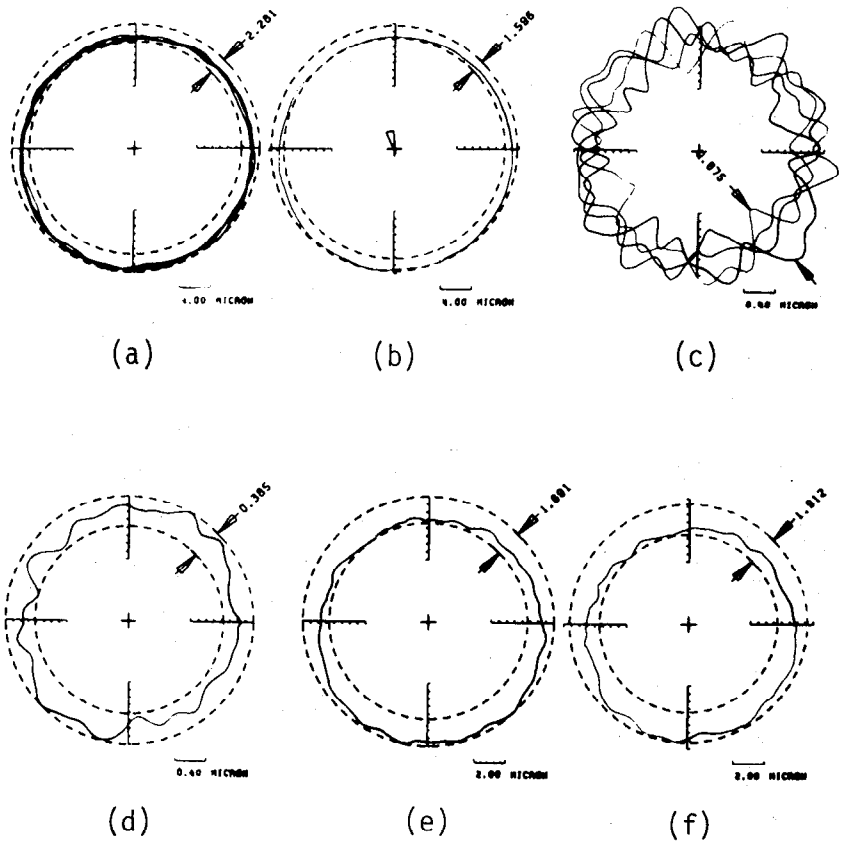

Fig. 22. Polar plots showing axial error motion of a spindle on conical roller bearings, fundamental amplitude = 0.71 and fundamental phase = -75.50: (a) polar plot; (b) average error motion; (c) random error motion; (d) residual error motion; (e) outer error motion; (f) inner error motion.

8. Rotating Sensitive Direction (Fixed Workpiece)

8.1 Principle

In contrast to lathes, cylindrical grinding machines, etc., jig borers represent another basic type of machine in which the workpiece is fixed and the cutting tool or gauge rotates. Out-of-roundness measuring machines, such as the Talyrond, are also in this category.

Since the sensitive direction is along a line going through the tool nose (or gauging point); in these machines, the sensitive direction rotates with the tool or the gauge.

The most logical solution for the detection of the radial error motion would be to fix the gauge radially on the rotating spindle and to mount the spherical marker on the workpiece (Fig. 23). The display on the screen of the oscilloscope and the

compensation of the master's eccentricity can be done with the same electronic circuit as described for the fixed sensitive direction. This setup is not advisable for higher speeds because the gauge support has a low stiffness. The low stiffness is due to several factors: (1) the gauge support must be provided with an element for the adjustment of the gap between the gauge and the master ball, (2) the setup creates a significant imbalance, and (3) the transmission of the capacitive-gauge signals through clip-rings is quite difficult.

For high speeds the most commonly used apparatus is that proposed by J. Tlusty (Fig. 24). A horizontal and vertical gauge fixed on the table sense radially against the master ball, which is mounted on the spindle with a small offset. The gauge output signals are amplified and fed to the respective horizontal and vertical inputs of an oscilloscope (Fig. 24).

The components of the motion signals, due to the offset of the spherical master, generate a circle on the screen of the

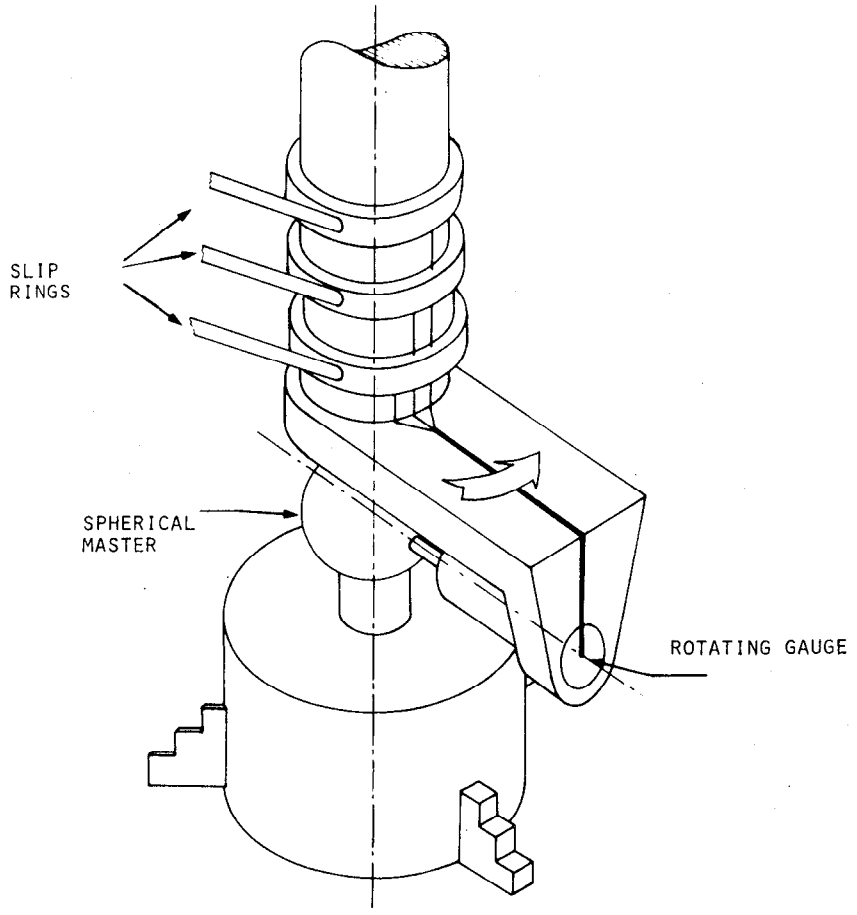

Fig. 23. Setup with rotating sensitive direction for measuring radial error motion.

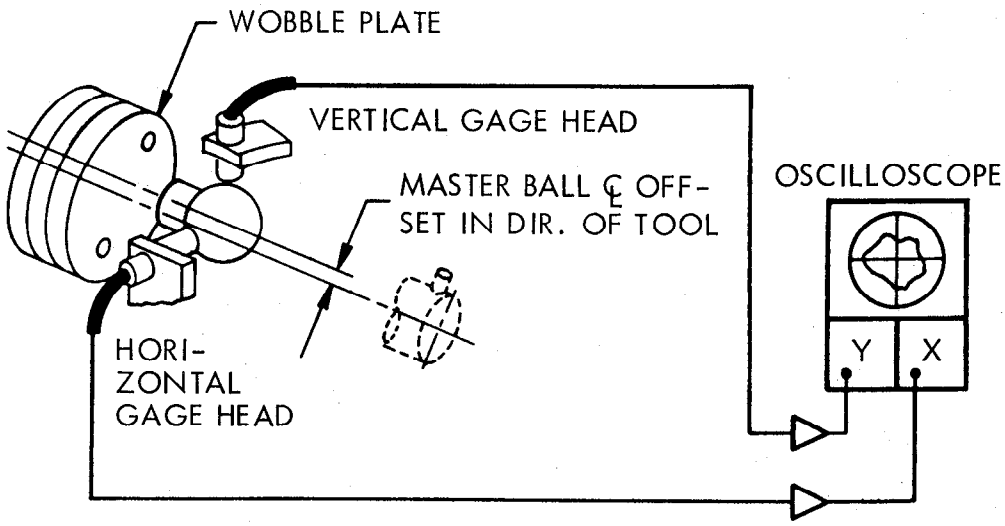

Fig. 24. Test method using a rotating sensitive direction for measuring radial error motion.

oscilloscope. The radial error motions in the direction of the master ball eccentricity are radially superimposed on this circle. Motions perpendicular to the master ball eccentricity move the spot on the screen tangentially to the base circle, causing a negligible effect on the shape. Thus, this arrangement yields a measurement of radial motion along a rotating sensitive direction, which is parallel to a line joining the axis average line with the geometrical center of the eccentric spherical master.

However, this setup is not valid for fixed sensitive directions as for lathes, cylindrical grinding machines, etc.

The difficulty in the method described above is the mechanical adjustment of the offset of the master ball. The offset direction must be parallel to the sensitive direction. If the distance between the center of the ball and the axis of rotation is too large, the diameter of the base circle will be so large that the departure from circularity of the figure on the screen can no longer be measured. If this distance is too small, the figure on the screen is completely deformed due to the crossings through the polar chart center.

It is possible, however, to generate the base circle with a vector resolver, as proposed by P. Vanherck. The error motion signals, detected on a centered master ball, can be superimposed on this base circle using an electronic device.

The setup for measuring the axial error motions for machines with rotating sensitive directions is identical to the one described for the fixed sensitive direction.

8.2 Typical Examples of Radial Error Motions with Rotating Sensitive Direction

Figure 25 shows a typical example of the radial error motion of a 3-kW jig borer. The error motion showed an ovality in the same direction, at all speeds. An analysis of the machine showed that the radial stiffness of the spindle in its bearing depended strongly on the direction in which the load was applied. The direction with the lowest stiffness coincided with the axis of ovality of the error-motion polar plot.

It is also possible to use a digital method for rotating sensitive direction. A typical example is shown in Fig. 26. The digital method has the capability of simulating all different angular tool positions with respect to the rotating spindle, from one single set of recorded motions. After digital compensation of the master ball's eccentricity, the total error motion value was found to be 3.2 μm. The average error motion value is 2.48 μm.

On the same figure the two gauge signals are represented in rectangular coordinates to prove that the error motion value, which can easily be evaluated from a polar plot, can hardly be deduced from rectangular coordinates.

9. Elimination of the Spherical-Master Roundness Error

9.1 Principle

A difficulty arises when the error motion of the spindle is of the same order or smaller than the out-of-roundness of the spherical master. It is, however, possible to separate the two sources of error by the method proposed by R. Donaldson [5].

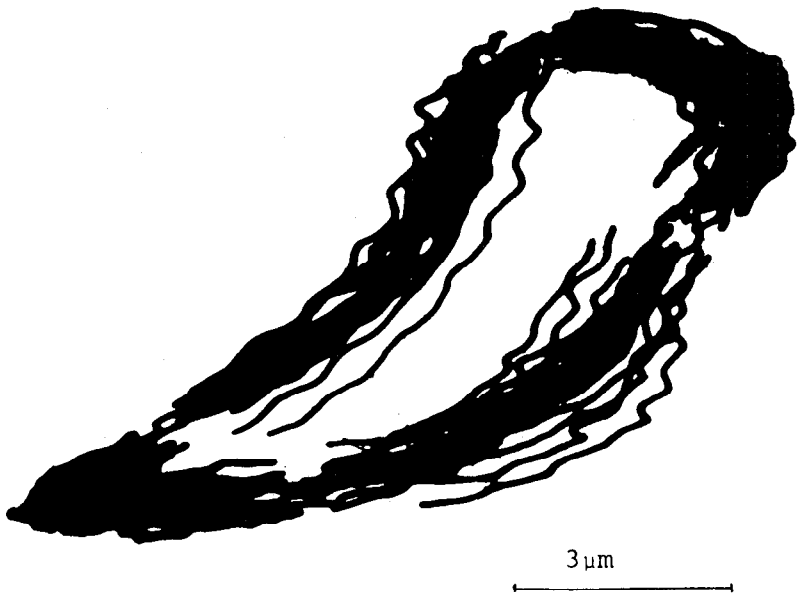

Fig. 25. Radial-motion polar plot of a jig borer.

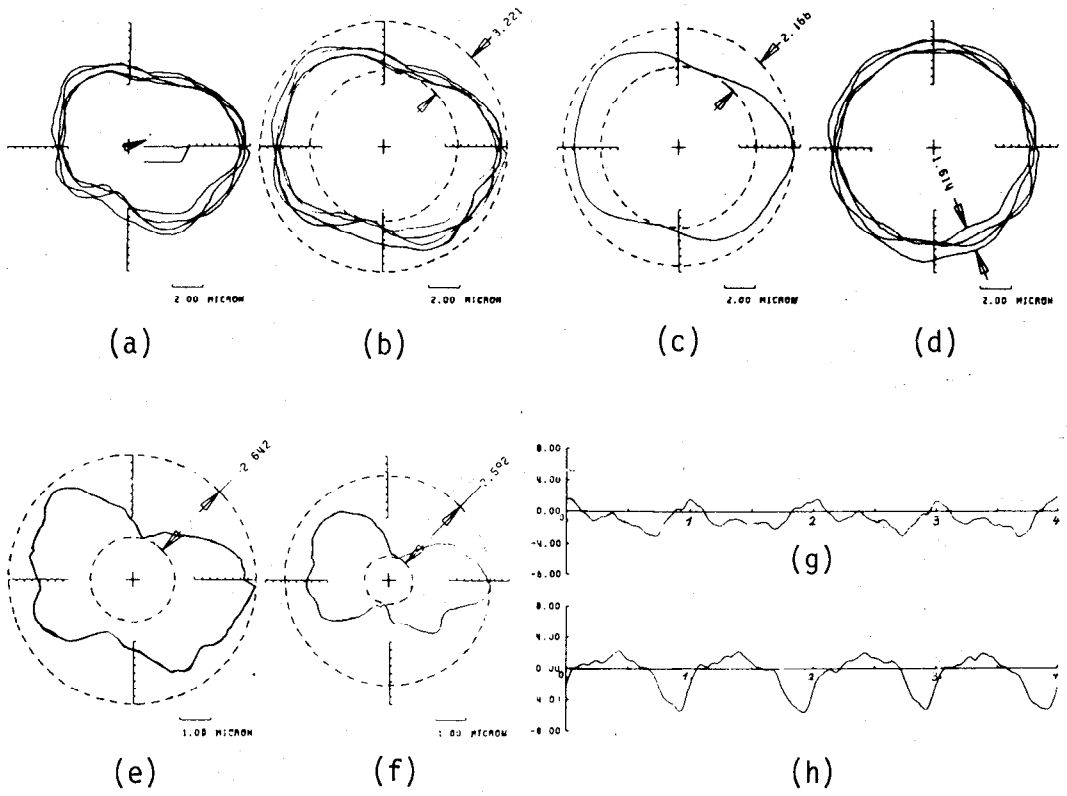

Fig. 26. Radial motion of a jig borer using a digital method, fundamental amplitude = 1.22 and fundamental phase = 18.34: (a) polar plot of total motion; (b) polar plot of total error motion; (c) polar plot of average error motion; (d) polar plot of random error motion; (e) polar plot of outer error motion; (f) polar plot of inner error motion; (g) output signal of gauge X; (h) output signal of gauge Y.

Two measurement setups are required as shown schematically in Fig. 27. Arbitrary initial positions are marked as $\theta = 0°$ by coincident marks on the part (test ball), spindle shaft, and spindle housing at the stylus position as shown in Fig. 27a. An initial polar record $T_1(\theta)$ is then made, using normal polarity (increasing chart radius corresponding to increasing part radius). In the second setup (Fig. 27b) the part and stylus positions have both been rotated 180° about the spindle axis while retaining the original shaft and housing positions. Two polar records are then made $T_{2P}(\theta)$ with normal polarity and $T_{2S}(\theta)$ with reversed polarity.

Using the above notation, it follows that relative to some base circle the initial record $T_1(\theta)$ can be expressed as

$$T_1(\theta) = P(\theta) + S(\theta) \qquad (2)$$

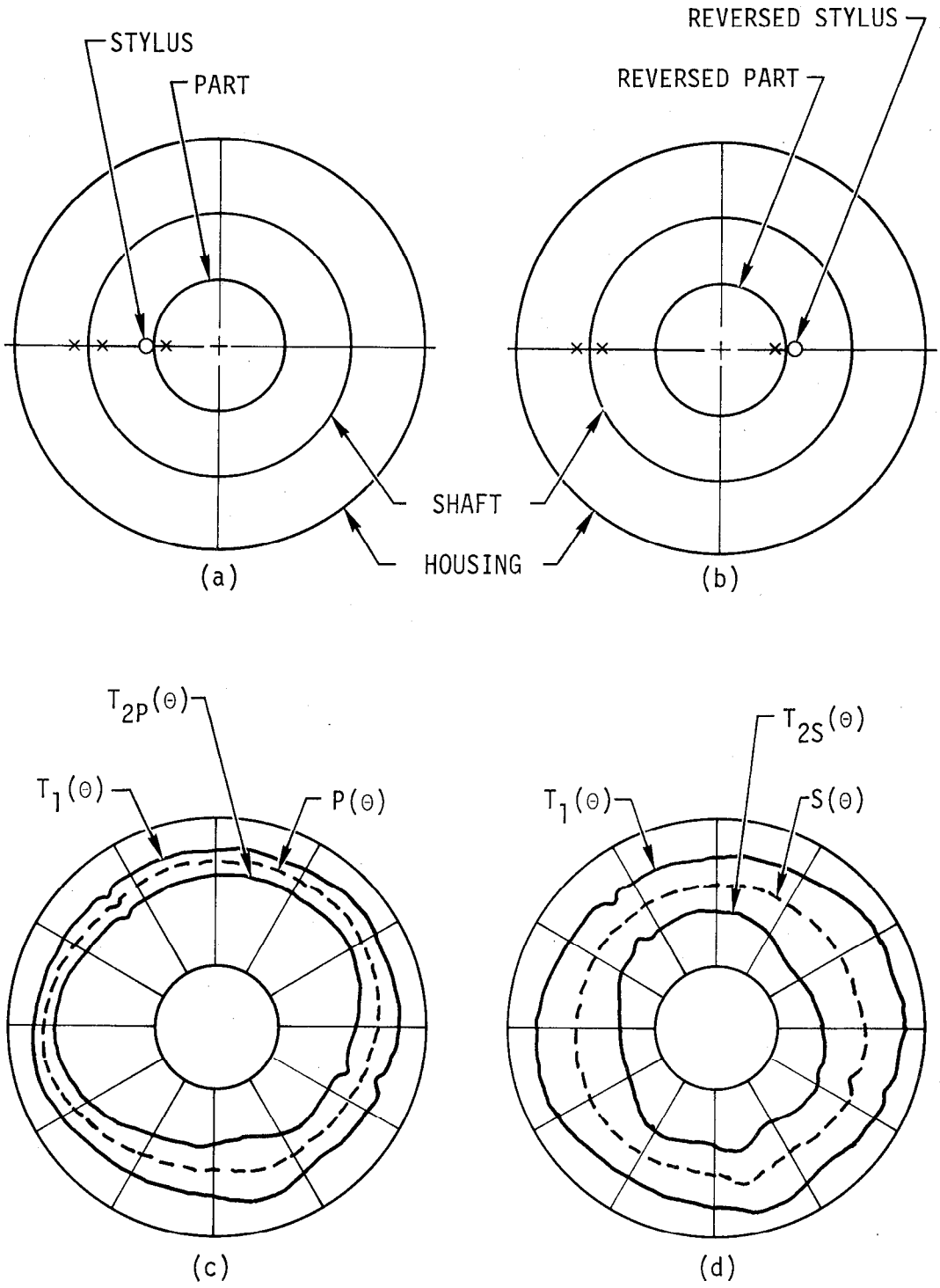

Fig. 27. Schematic test setups for (a) $T_1(\theta)$ and (b) $T_{2P}(\theta)$ and $T_{2S}(\theta)$, and error separation by profile averaging for (c) part profile $P(\theta)$ and (d) spindle error $S(\theta)$ (taken from Ref. 5).

In Fig. 27b, the unchanged relative position of the part and stylus yields the same $P(\theta)$ profile. However, axis motion toward the stylus in Fig. 27a becomes motion away from the stylus in Fig. 27b, so that

$$T_{2P}(\theta) = P(\theta) - S(\theta) \qquad (3)$$

The polarity reversal from $T_{2P}(\theta)$ to $T_{2S}(\theta)$ yields

$$T_{2S}(\theta) = - P(\theta) + S(\theta) \qquad (4)$$

Adding Eqs. (1) and (2) and then Eqs. (1) and (3) yields

$$P(\theta) = 1/2 \left[T_1(\theta) + T_{2P}(\theta)\right] \qquad (5)$$

$$S(\theta) = 1/2 \left[T_1(\theta) + T_{2S}(\theta)\right] \qquad (6)$$

Thus by recording $T_1(\theta)$ and $T_{2P}(\theta)$ on the same polar chart the part roundness error profile $P(\theta)$ is obtained by simply drawing a third average profile halfway between the first two, as shown in Fig. 27c. The same profile averaging procedure can be used to obtain the spindle radial motion error profile $S(\theta)$ from a chart containing $T_1(\theta)$ and $T_{2S}(\theta)$ (see Fig. 27d). The values of roundness and radial motion errors can be assessed by means of one of the methods involving concentric circles about a best fit center (minimum radial separation, least squares, etc.). The error values are not influenced by different base circle radii or different centering errors (limited only by polar distortion) for the various measurements. The method is only applicable to the repeatable, or average, portion of the error motion.

9.2 Actual Example of a Master Roundness Elimination

The radial error motion of the axis of rotation of a roundness measuring machine with rotating stylus was measured with a glass spherical master having roundness errors of the same order as the error motion of the spindle.

The Donaldson eliminating method has been used with digital recording and computation.

A homemade rotational recorder, consisting of a disk with 64 equispaced holes, was fixed on the spindle. The frequency of the encoder output signal was multiplied by 16, using a ratio tuner to obtain 1024 samples per revolution. A single slot in the border of the disk was used to start the sampling period at the zero-degree reference position.

The average error motion has been computed over these revolutions. The fundamental component, due to the eccentricity of the spherical master and the shift, due to thermal shift, were

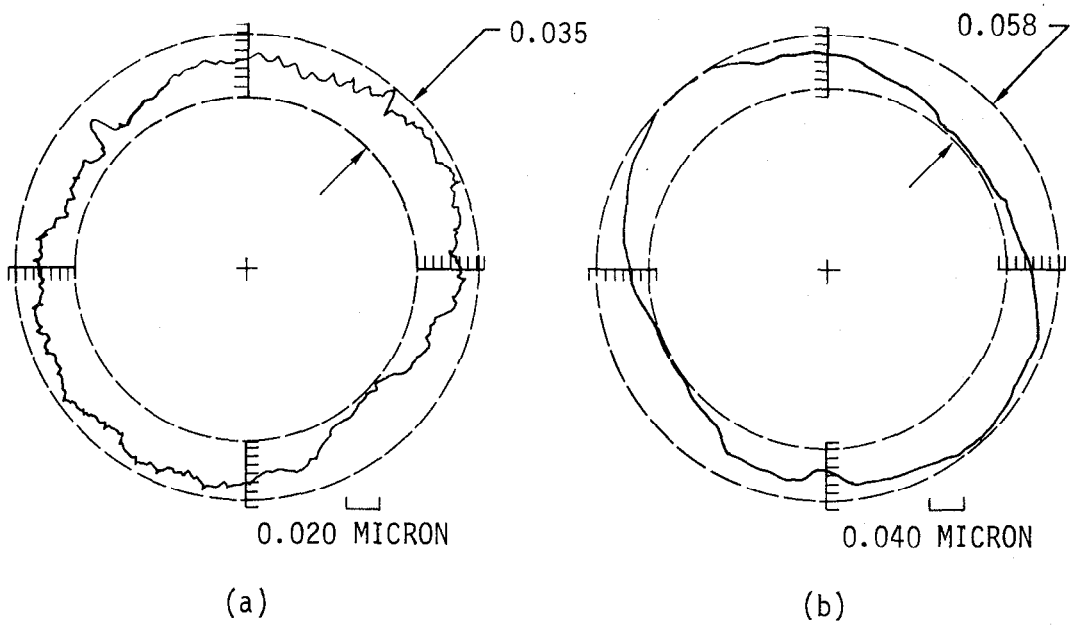

Fig. 28. Example of eliminating the master roundness error: polar plots showing (a) spindle radial error motion and (b) spherical master profile.

removed digitally. The correct 180° rotation of the master, for the second step, was checked by a light beam and mirrors.

The sum of the averages of the two steps yields the radial error motion of the spindle (shown in Fig. 28a) with a total error motion value from the least square center of 0.035 μm. The difference between the two average signals yields the roundness error of the spherical master with an out-of-roundness from the L.S.C. of 0.058 μm (Fig. 28b).

To check the validity of the results the spherical master was rotated 90° about the axis of rotation and the complete test procedure repeated. This second axis-of-rotation error-motion polar plot had the same shape as the first one and a total error motion value of 0.033 μm.

It can be concluded that even when the out-of-roundness of the master is 70% larger than the error motion, and at the same time a significant thermal drift is present, the axis of rotation motion can be evaluated with a precision of 0.002 μm for a total error motion of 0.034 μm.

When the digital method is used, the out-of-roundness error of the spherical master can be stored in memory, so the error motion of an axis can be evaluated in one step.

10. Comparison of the Measurement of the Error Motion of Axes of Rotation and the Tests Prescribed by ISO R 230 (1961)

Concerning the radial direction, the ISO recommendation proposes to measure the out-of-true running (run-out) of a component at a given axial position (5.6). "The plunger of a dial gauge is brought in contact with the revolving surface to be tested and the readings of the instrument observed while the spindle is slowly rotated through one turn" (5.612.2).

The run-out is evaluated as the difference between the maximum and minimum reading of the instrument.

"In general this measured run-out is the result of:

- The radial throw of the axis (the difference between the geometrical axis of the component and the rotating axis in the considered section).
- The out-of-roundness of the component.
- The errors in the bearings." (5.611.4)

This means that a spindle with a small axis-of-rotation error motion and capable of producing workpieces with cross sections with a high degree of circularity, could, due to the out-of-roundness and the radial throw of the spindle nose, present a significant run-out.

On the other hand, when the component on which the run-out is measured (e.g., the spindle nose) has been ground on the spindle in its bearings, the run-out could be very low even with a significant axis-of-rotation error motion.

The run-out, detected on low speed rotating spindles, does not include the error motions due to structural vibrations excited by unbalances, belts, etc.; neither does it include the behavior of the bearings in the actual working conditions.

The same comments can be made concerning the axial direction. The ISO 230 recommends measuring at a low speed the camming of a component.

"Camming is the resultant of various defects of the surface and axis of rotation: (a) surface not flat (b) surface and axis of rotation not perpendicular, and (c) periodic displacement of the axis" (ISO R 230/5.631.1).

The error motion of axes of rotation, however, have to be carried out at the actual working speed of the machine. This means that the actual behavior for finishing operations of the bearings and the structural deformations are included. On the other hand, the polar representation permits the separation of the error motions appearing in synchronism with the spindle rotation and generating form errors of the machined workpiece, and the nonsynchronized error motions which cause surface roughness.

It is generally possible to deduce from the shape of the polar plot the source of the error motion.

It can be concluded that the ISO R 230 does not prescribe tests for the measurement of error motions of axes of rotation in actual working conditions. The tests proposed by ISO R 230 are, however, quite valuable for the determination of the run-out of rotating elements. This yields the conclusion that both tests are completely complementary.

References

Cited

1. J. Tlusty, System and Methods of Testing Machine Tools, Microtechnic, vol. 13 (1959) 162.

2. J. B. Bryan, R. W. Clouser, and E. Holland, Spindle Accuracy, American Machinist, December 4, 1967.

3. ANSI Standard B89.3.4 - 197X, Axes of Rotation October 1973.

4. J. Peters and P. Vanherck, An Axis of Rotation Analyser, Proceedings of the 14th International MTDR Conference, Manchester 1973, Pergamon Press, Oxford.

5. R. R. Donaldson, A Simple Method for Separating Spindle Error from Test Ball Roundness Error, Annals of the CIRP, vol. 21-1 (1972) 125-126.

Uncited

M. Boets and K. Knops, Foutbewegingen op Rotatieassen — Digitale Methode, Thesis 74E4, Instituut voor Wektuigkunde, Katholieke Universiteit Lewven, 1974.

Koenigsberger and J. Tlusty, Specifications and Tests for Metal Cutting Machine Tools, UMIST.

Vanek, Measurement of Accuracy of Rotation of Machine Tool Spindle, VUOSO, 1969.

Vanek, Metody a Hodnoceni Mereni Presnos ti Otaceni Vreten Obrabecich Stroju, VUOSO, 1971.

P. Vanherck, Error Motion of Axes of Rotation Analog or Digital Measurement, Proceedings of the Int. Conf. on Prod. Engineering, Tokyo, 1974, p. 445-450.

P. Vanherck and J. Peters, Digital Axis of Rotation Measurements, Annals of the CIRP, vol. 22-1, 1973.

P. Vanherck and J. Peters, Messung des Bewegungsfehlers der Rotationsachse, Werkstatt und Betrieb 106 (1973) 9.

Printed in the United States of America
Available from
National Technical Information Service
U. S. Department of Commerce
5285 Port Royal Road
Springfield, Virginia 22151
Price: Printed Copy $___*; Microfiche $2.25

*Pages	NTIS Selling Price
1-50	$4.00
51-150	$5.45
151-325	$7.60
326-500	$10.60
501-1000	$13.60